Supramolecular Chemistry
Publication details, including instructions for authors and subscription information:
http://www.informaworld.com/smpp/title~content=t713649759

Pyridyl-, bipyridyl-, and terpyridyl-functionalised azamacrocycles

Nathaniel W. Alcock[a]; Adam J. Clarke[a]; William Errington[a]; Ana Maria Josceanu[a]; Peter Moore[a]; Simon C. Rawle[a]; Philippa Sheldon[a]; Stephen M. Smith[a]; Mary L. Turonek[a]
[a] Department of Chemistry, University of Warwick, Coventry, UK

To cite this Article Alcock, Nathaniel W. , Clarke, Adam J. , Errington, William , Josceanu, Ana Maria , Moore, Peter , Rawle, Simon C. , Sheldon, Philippa , Smith, Stephen M. and Turonek, Mary L.(1996) 'Pyridyl-, bipyridyl-, and terpyridyl-functionalised azamacrocycles', Supramolecular Chemistry, 6: 3, 281 — 291
To link to this Article: DOI: 10.1080/10610279608032546
URL: http://dx.doi.org/10.1080/10610279608032546

SUPRAMOLECULAR CHEMISTRY, Vol. 6, pp. 281–291
Reprints available directly from the publisher
Photocopying permitted by license only

Pyridyl-, bipyridyl-, and terpyridyl-functionalised azamacrocycles

NATHANIEL W. ALCOCK, ADAM J. CLARKE, WILLIAM ERRINGTON, ANA MARIA JOSCEANU, PETER MOORE*, SIMON C. RAWLE, PHILIPPA SHELDON, STEPHEN M. SMITH and MARY L. TURONEK

Department of Chemistry, University of Warwick, Coventry CV4 7AL, UK

(Received June 13, 1994)

A series of azamacrocycles which have been *N*-functionalised with pendent pyridylmethyl-(*py*CH_2-), bipyridylmethyl-(*bipy*CH_2-) and terpyridylmethyl- (*terpy*CH_2-) arms have been synthesised and characterised, and some of their coordination chemistry with transition metal ions is reported. By attaching the pendent-arms at the 5- rather than the 6-position of the *py*, *bipy* and *terpy*, new ligands are generated which can be used to form polynuclear metal complexes *in a controlled and systematic fashion*. Fluorescent pH and transition metal ion sensors have been developed by reacting the azamacrocyclic N-pendent *bipy*CH_2 arm(s) with *cis*-[Ru(*bipy*)$_2$Cl$_2$], to give macrocycles with up to four attached [Ru(*bipy*)$_3$]$^{2+}$ groups. That based on 1,4,7-triazacyclononane (9N3), with three attached [Ru(*bipy*)$_3$]$^{2+}$ groups, has a first photo excited state pK_a of 7.1, and is a useful fluorescent sensor for physiological pH at below micromolar concentrations. The analogous derivative of *cyclam* (1,4,8,11-tetraazacyclotetradecane) carrying four [Ru(*bipy*)$_3$]$^{2+}$ groups has a first photo excited state pK_a of 5.7, allowing kinetic and thermodynamic fluorescence studies of metal ion uptake by an azamacrocycle at neutral pH without complications from protonated species. A *pre-organised* hexadentate tris(2,2′-bipyridyl) chelating ligand, 1,4,7-tris(2′,2″-bipyridyl-5′-ylmethyl)-1,4,7-triazacyclononane (L) has been developed, and crystal structures of mononuclear complexes [M(LH)]$^{3+}$ (M = Ru, Cu) are reported. In [M(LH)]$^{3+}$ the azamacrocyclic N-atoms are non-coordinating to M, but have a very high affinity for a single proton trapped in the macrocyclic cavity. An analogous and potentially nonadentate ligand has been developed based on 9N3 with three N-pendent *terpy*CH_2-arms.

INTRODUCTION

Studies of pendent-arm macrocycles and their metal complexes continue to attract significant attention. Such ligands combine the advantages of a macrocyclic framework with the added flexibility of the attached pendent-arm(s). When the pendent-arms are positioned so that coordination to a single metal ion can occur at both the macrocyclic centre and at the pendent-arm(s) (*e.g.* $\mathbf{L^1}$ and $\mathbf{L^2}$), extra stability results from the increased ligand denticity. Furthermore, the pendent-arms can enhance the rate, and control the mechanism, of metal ion uptake. For example, the *bipy*-pendent macrocycles $\mathbf{L^1}$ and $\mathbf{L^2}$ (*bipy* = 2,2′-bipyridine) have been shown to capture a transition metal ion at the pendent-arm, prior to coordination of the metal ion by the macrocycle.[1]

The pendent-arms can also be used to help define the metal ion stereochemistry, which is an important aspect in developing ligands which form complexes with a preferred coordination geometry.[2,3] In designing macrocycles for a particular metal ion stereochemistry, the demands of the metal ions also need to be taken into account. For example, whereas $\mathbf{L^1}$ was found to give a five-coordinate distorted trigonal bipyramidal $[Zn(\mathbf{L^1})]^{2+}$, the preference of Ni^{2+} is to form a six-coordinate pseudo-octahedral $[Ni(\mathbf{L^1})OH_2]^{2+}$ ion.[4] Similarly, we have found that $\mathbf{L^4}$ and $\mathbf{L^5}$, with three carbon linked *N*-pendent arms, give the tetrahedral $[Zn(\mathbf{L})]^{2+}$ ($\mathbf{L}$ = $\mathbf{L^4}$ and $\mathbf{L^5}$),[2,3] whereas Ni^{2+} forms the six-coordinate species $[Ni(\mathbf{L^6})(NCS)_2]$. Ni^{2+} also forms a binuclear, antiferromagnetically coupled $[\{(HL^4)Ni(NCS)\}_2CO_3]^{2+}$, which has a protonated non-coordinating pendent-arm and an unusual doubly bridging carbonate ion.[5] The preference of Ni^{2+} for six-coordination can be traced to

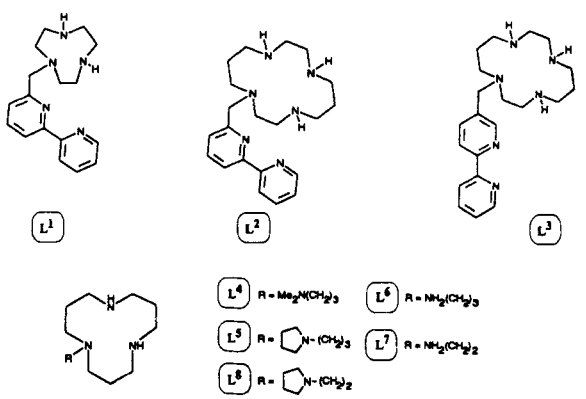

*To whom correspondence should be addressed.

its d^8 electronic configuration, and the enhanced ligand-field stabilisation energy that this geometry produces. The d^{10} electronic configuration of Zn^{2+} avoids ligand-field effects, and then the stereochemical preferences of the pendent-arm ligands becomes more evident. For example, with Zn(II) the shorter (two carbon linked) pendent-arm macrocycles $\mathbf{L^7}$ and $\mathbf{L^8}$ cannot use their pendent arms to span the metal to give a tetrahedral complex, and instead form five-coordinate complexes of the type $[Zn(\mathbf{L})OClO_3]^+$ ($\mathbf{L} = \mathbf{L^7}$, $\mathbf{L^8}$), with a unidentate perchlorate group occupying the fifth coordination site.[2,3]

The use of pendent-arm macrocycles can be anticipated to become important in developing catalysts with a well ordered metal stereochemistry (*e.g.* complexes with two vacant, labile *cis*-coordination sites are often required for substrate uptake and catalytic reactions).[6] The higher lability of the pendent arms compared with the relative inertness of the macrocyclic metal-ligand bonds may also be important in this respect.

Attachment of several pendent-arms to an azamacrocycle can also result in the formation of binuclear metal complexes, with the macrocycle sometimes adopting an 'exo' conformation. An early example of this type of behaviour was shown for the 1,4,8,11-tetrakis(2'-pyridylmethyl)-1,4,8,11-tetraazacyclotetradecane ($\mathbf{L^9}$). This gives the binuclear, centrosymmetric complex $[(BrCu)_2(\mathbf{L^9})]^{2+}$, in which each Cu(II) has a distorted square-pyramidal geometry with coordination to two adjacent pyridyl arms, the two corresponding adjacent azamacrocyclic N-atoms (in this case either the 1,4 or the 8,11 pairs of *cyclam* N-atoms) and one bromide ion.[7]

An alternative strategy for forming polynuclear metal complexes with pendent-arm azamacrocycles is illustrated by *bipy* pendent-arm ligand $\mathbf{L^3}$. In $\mathbf{L^3}$, attachment of the bipyridyl arm at the 5-position of the *bipy*, rather than at the 6-position (as in $\mathbf{L^1}$ and $\mathbf{L^2}$), makes it sterically impossible for both the azamacrocycle and the *bipy* group to coordinate to a *single* metal ion.[8] $\mathbf{L^3}$ has been shown to react with equimolar concentrations of different divalent metal ions (M^{2+}) to give complexes in which the metal ions either enter the *cyclam* cavity (*e.g.*

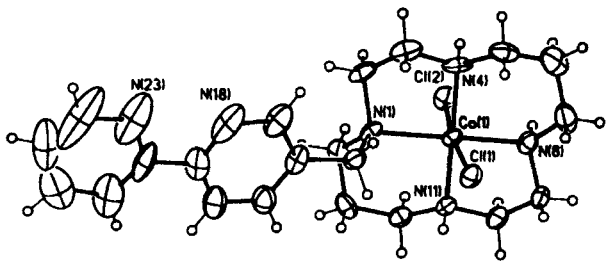

Figure 1 Crystal structure of *trans*-$[Co(\mathbf{L^3})Cl_2]^+$.

M = Co, Ni, Cu, Zn), or with Fe^{2+} to give the low-spin $[Fe(\mathbf{L^3})_3]^{2+}$ by reaction with the pendent *bipy* group (producing predominantly the *mer* isomer, $\mathbf{L^{11}}$). $CoCl_2$ reacts with $\mathbf{L^3}$ in the presence of O_2 to give the Co(III) complex *trans*-$[Co(\mathbf{L^3})Cl_2][ClO_4]$. The crystal structure (**Figure 1**) clearly shows the metal ion at the centre of the *cyclam* cavity, with the *bipy* arm uncoordinated.[9]

Reaction of $\mathbf{L^3}$ with *cis*-$[Ru(bipy_2)Cl_2]$ gives $\mathbf{L^{10}}$ (**Scheme 1**), and $\mathbf{L^{10}}$ reacts further with several divalent metal ions (M^{2+}) to give dinuclear species of the type $[(bipy)_2Ru(\mathbf{L^3}M)]^{4+}$. The three unoccupied *cyclam* groups of $\mathbf{L^{11}}$ are also available to give tetranuclear mixed-metal species of the type $[\{Fe(L^3M)_3\}]^{8+}$ (*e.g.* M = Ni, Cu), and the same tetranuclear mixed metal complexes may also be obtained by reaction of $\mathbf{L^{12}}$ or $\mathbf{L^{13}}$ with Fe^{2+}.[8]

$\mathbf{L^{10}}$ is strongly fluorescent like $[Ru(bipy)_3]^{2+}$ (λ_{ex} = 450 nm, λ_{em} = 600 nm), and this fluorescence is quenched significantly (but not completely) as cations such as Cu^{2+}, Ni^{2+} and $4H^+$ enter the macrocyclic cavity. Zn^{2+} does not affect this fluorescence significantly. Therefore, $\mathbf{L^{10}}$ is both a pH and selective transition metal ion sensor, and this aspect of a variety of related systems is explored in this study. Some of the new polynucleating ligands under investigation are $\mathbf{L^3}$ and $\mathbf{L^{14}}$-$\mathbf{L^{17}}$. $\mathbf{L^{10}}$, and the analogous mono-, bis-, tris- and tetrakis-$[Ru(bipy)_2\mathbf{L}]^{2+}$ analogues of $\mathbf{L^{14}}$-$\mathbf{L^{17}}$ ($\mathbf{L} = \mathbf{L^{14}}$-$\mathbf{L^{15}}$; R = B) are being investigated for their fluorescence pH and metal ion sensing properties, including thermodynamic and stopped-flow kinetic and mechanistic studies of labile metal ion uptake.

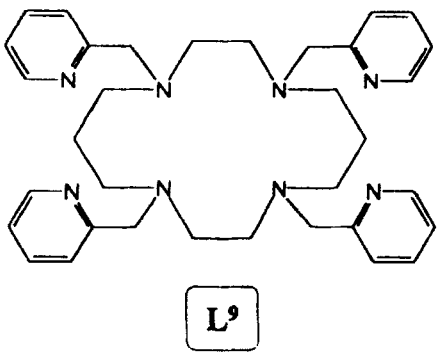

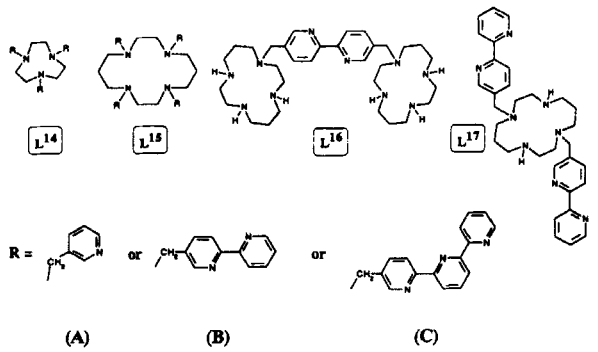

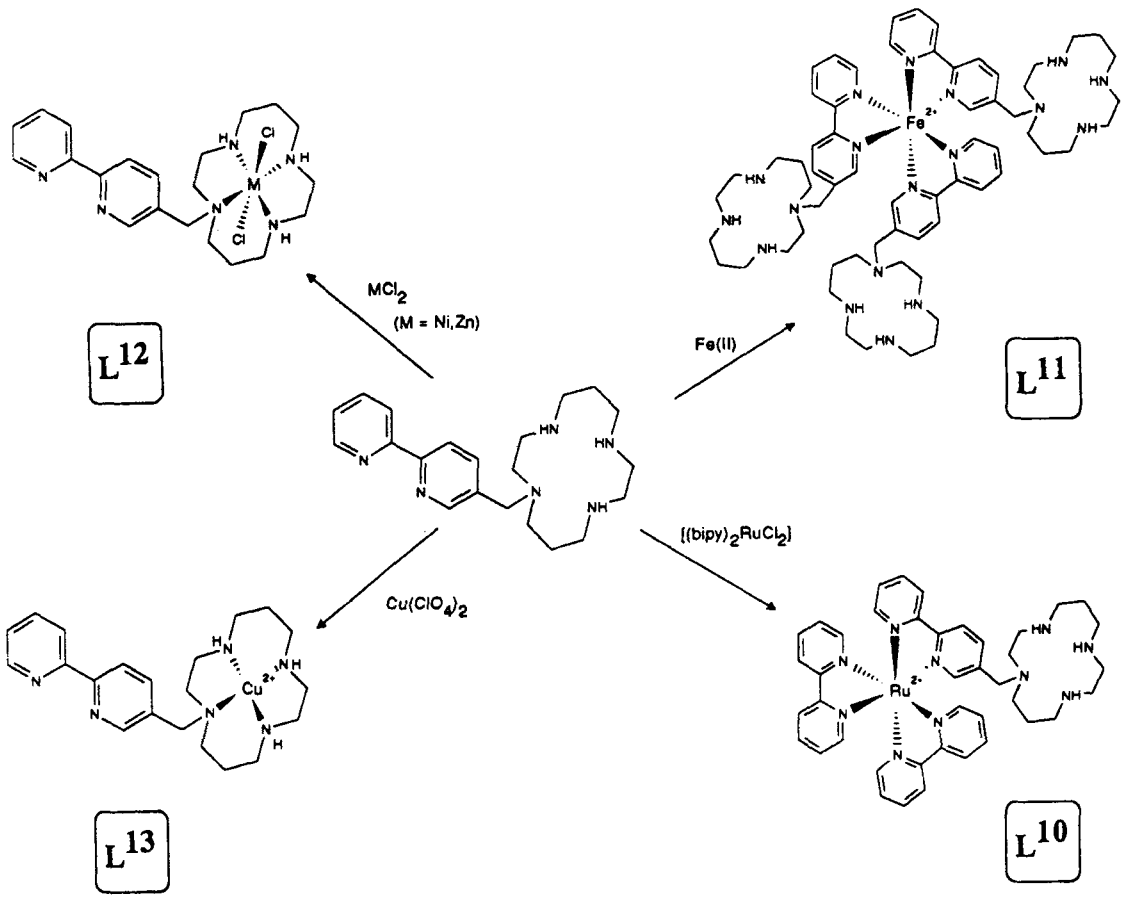

Scheme 1

Mononuclear complexes of the hexa- and nona-dentate ligands L^{14} (R = B and C respectively) have also been isolated as the monoprotonated $[M(L^{14}H)]^{3+}$ (M = Fe, Co, Ni, Cu, Zn and Ru, R = B) and $[M(L^{14})]^{3+}$ (M = La, Eu, R = C). Crystal structures of $[M(L^{14}H)]^{3+}$ (M = Cu and Ru) are also reported, showing that the azamacrocyclic N atoms are uncoordinated. ^1H NMR studies also reveal a tightly bound proton bonded to the 9N3. Molecular modelling studies show that L^{14} are *pre-organised* ligands for six-coordination (R = B) or ninecoordination (R = C). L^{16} forms tris chelates, $[M(L^{16})_3]^{2+}$ (M = Fe, Ru), which in turn react with other divalent metal ions (M′) to give the heptanuclear complexes $[M(L^{16}M'_2)_3]^{8+}$.

Synthesis of azamacrocycles with N-pendent pyridylmethyl-, bipyridylmethyl- and terpyridylmethyl-arms

Preparation of the fully N-alkylated azamacrocycles such as L^{14} and L^{15} is readily achieved by direct alkylation of the parent, unalkylated macrocycles with an excess of the requisite alkylating agent, $ArCH_2X$ (X = Cl, Br; Ar = aromatic group). An example is shown in **Scheme 2**. Such reactions are not possible with an excess of aliphatic alkyl halides, since quaternisation of the macrocyclic N-atoms occurs. This difficulty may be overcome by a different route which involves reaction of the

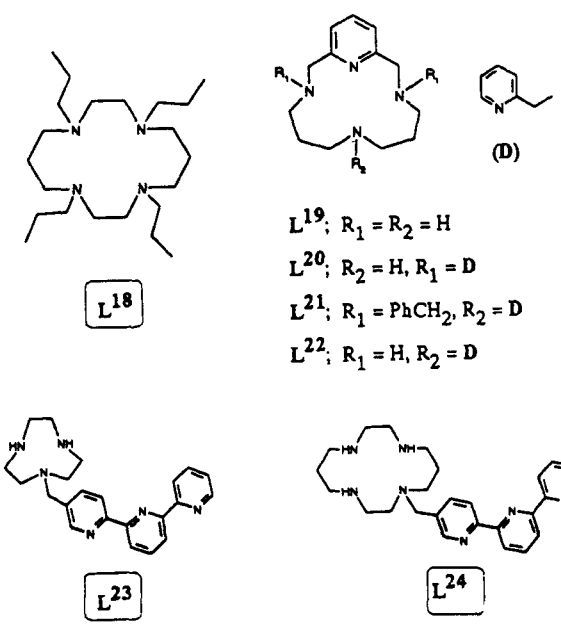

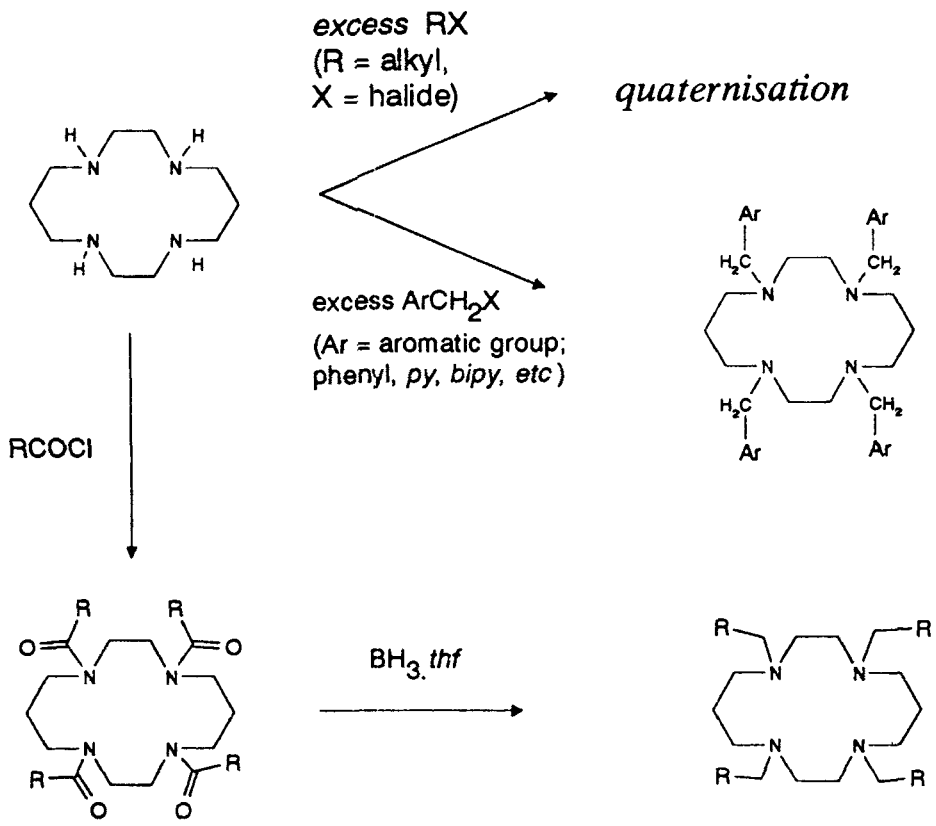

Scheme 2

parent macrocycles with acid chlorides, followed by reduction of the amide groups with BH_3.thf (**Scheme 2**).[9] The N-tetrapropyl *cyclam* $\mathbf{L^{18}}$ was obtained in this way, and found to give the unusual six coordinate complex *trans-R,S,R,S*-[Ni($\mathbf{L^{18}}$)$(NCS)_2$].[10] *R,S,R,S*-[Ni(*tmc*)]$^{2+}$ (*tmc* = 1,4,8,11-tetramethyl-1,4,8,11-tetraazacyclotetradecane) more commonly gives five-coordinate complexes of the type [Ni(*tmc*)X]$^+$ (X = NCS, Cl, N_3).

The alkylating agent 5-bromomethyl-2,2′:6′:2″-terpyridine required to obtain $\mathbf{L^{14}}$ and $\mathbf{L^{15}}$ (R = C), and the monofunctionalised polynucleating macrocycles $\mathbf{L^{23}}$ and $\mathbf{L^{24}}$, is obtained from the photo catalysed reaction of 5-methyl-2,2′:6′:2″-terpyridine and *N*-bromosuccinimide. The synthesis of 5-methyl-2,2′:6′:2″-terpyridine is outlined in **Scheme 3**.

Sometimes direct alkylation of azamacrocycles with an excess of $ArCH_2X$ does not lead to complete N-alkylation, and this behaviour, which can be traced to steric effects, is useful for selective substitution. For example, reaction of $\mathbf{L^{19}}$ with benzyl chloride under mild conditions produces the dibenzyl derivative (R_1 = CH_2Ph, R_2 = H), and further reaction of this dibenzyl derivative with 2-chloromethylpyridine under more forcing conditions gives the mono(2-pyridylmethyl) derivative $\mathbf{L^{21}}$.[10] Similarly, reaction of $\mathbf{L^{19}}$ with 2 mole equivalents of 2-chloromethylpyridine, in a two phase

Synthesis of 5-methyl-2,2′:6′,2″-terpyridine

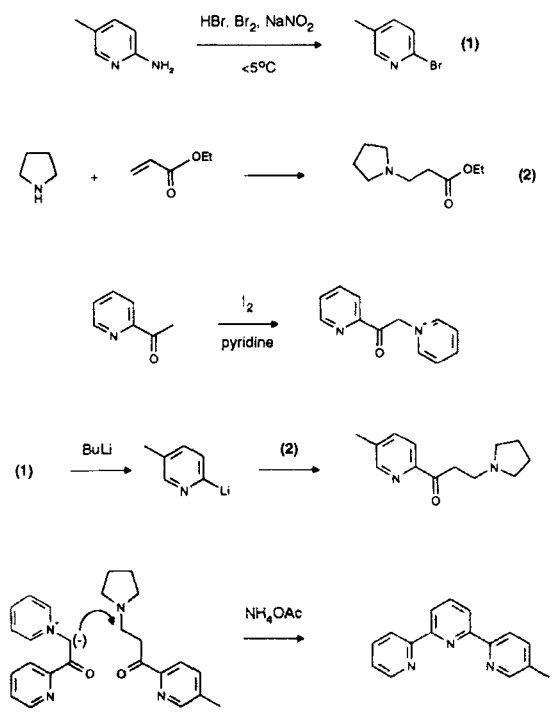

Scheme 3

Synthesis of L^{22} and its Dimethyl Derivative

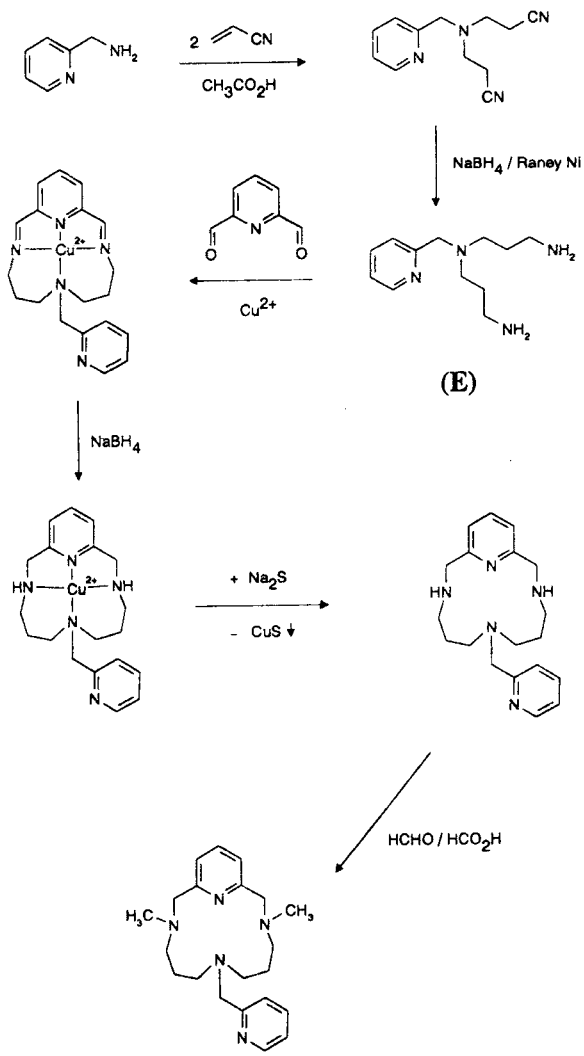

Scheme 4

aqueous base/dichloromethane reaction, gives the hexadentate di(2-pyridylmethyl)-derivative, L^{20}.[11] L^{20} forms six-coordinate complexes such as *cis*-$[Ni(L^{20})]^{2+}$ in which the macrocycle is folded about an axis defined by the two N-atoms carrying the R_1 groups. The ease of N-alkylation of the two secondary amino groups which flank the pyridine of L^{19}, and the more difficult N-alkylation of the third NH-group, arises from the structure of the parent macrocycle which has the lone pairs of NR_1 pointing 'exo', and that of NR_2 pointing 'endo'. The latter is therefore less accessible for nucleophilic attack at an alkyl halide.[10,11]

Mono-N-alkylation of a tri- or tetra-azamacrocycles may also be achieved either by reaction of the alkylating agent with an excess of macrocycle,[8] or by incorporating the single pendent-arm into one of the synthons prior to macrocyclic ring formation. L^{22}, which cannot be obtained by the selective alkylation route described above, has recently been made by the Cu^{2+} template synthetic route outlined in **Scheme 4**.[12] The synthon (**E**) required to introduce the 2-pyridylmethyl pendent arm is obtained from 2-aminomethylpyridine, by reaction with two moles of acrylonitrile using an acetic acid catalyst, followed by reduction of the two terminal nitrile groups with sodium tetrahydroborate and Raney nickel. (**E**) is then converted to the required pendent-arm macrocycle by a Cu^{2+} template synthesis with pyridine-2,6-dicarbaldehyde, followed by reduction of the two imine bonds with sodium tetrahydroborate, and removal of the Cu^{2+} with sulfide in the usual way. L^{22} may be readily methylated at the two remaining secondary amino groups using formaldehyde and formic acid,[12] and further alkylations using the route shown in **Scheme 2** will be possible.

The intermediate (**E**) (**Scheme 4**) may also be used in a Richman-Atkins synthesis of 1-(2′-pyridylmethyl)-1,5,9-triazacyclododecane as outlined in **Scheme 5**. 1-(2′-pyridylethyl)-1,5,9-triazacyclododecane has also been obtained in this way.[13]

Flourescent pH and metal ion sensors

The macrocycles L^{10}, and L^{25}-L^{27} all show a strong fluorescence at high pH, and this fluorescence is markedly quenched as cations bind to the azamacrocycles. A comparison of the fluorescent spectra of $[Ru(bipy)_3]^{2+}$ (8×10^{-6} mol dm^{-3}) with L^{27} (2×10^{-6} mol dm^{-3}) at high pH is shown in **Figure 2**. Also shown in **Figure 2** is quenching effect of adding strong acid or excess Ni^{2+} and Cu^{2+} to L^{27}. Similar quenching is not observed when

Synthesis of 1-(2'-Pyridylmethyl)-1,5,9-triazacyclododecane, and its 5,9-dimethyl derivative

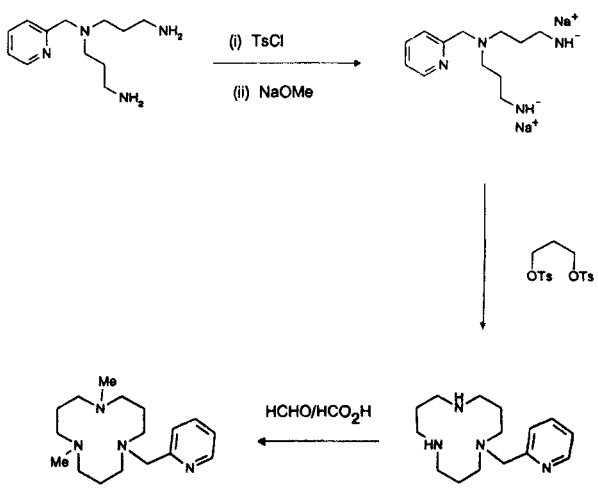

Scheme 5

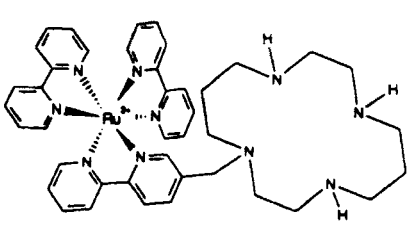

L^{10}

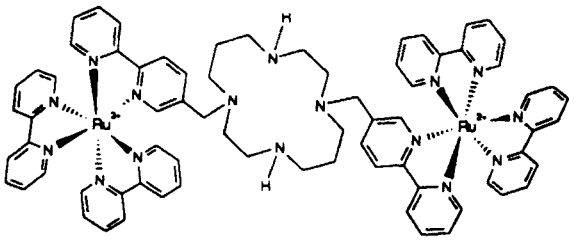

L^{25}

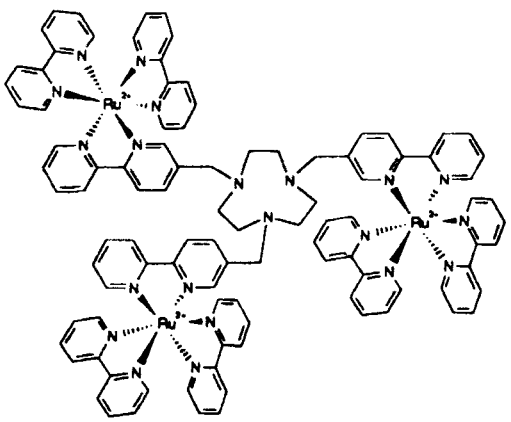

L^{26}

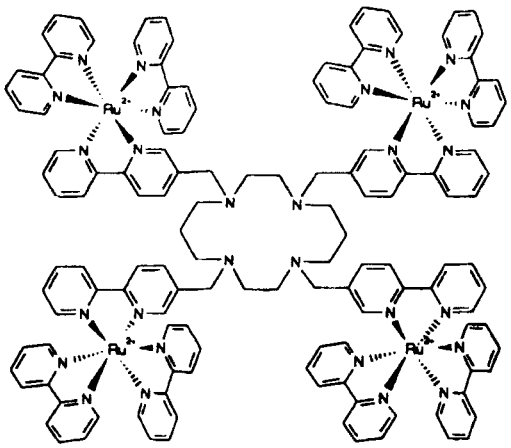

L^{27}

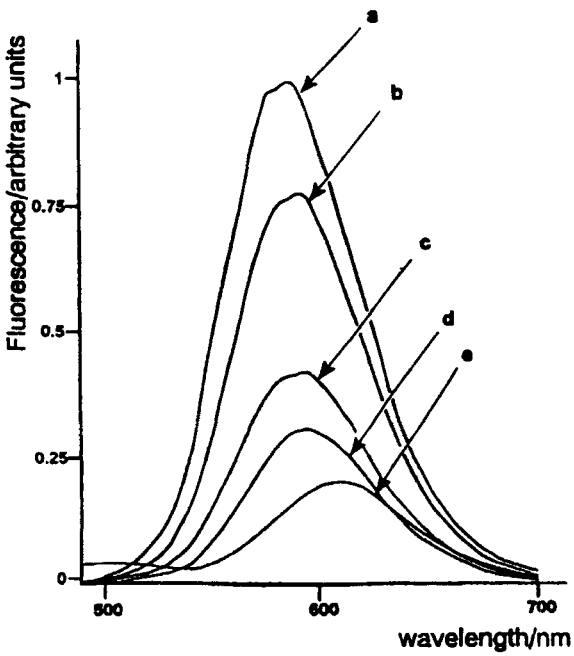

Figure 2 Quenching of the fluorescence spectrum of 1,4,8,11-tetrakis{bis(2′,2″-bipyridyl)(2′,2″-bipyridyl-5′-yl-methyl)ruthenium-(II)}-1,4,8,11-tetraazacyclotetradecane (L^{27}; 2×10^{-6} mol dm^{-3}; spectrum (b); λ_{ex} 450 nm), upon addition of excess (e) H^+, (d) Cu^{2+}, and (c) Ni^{2+} ions. Spectrum (a) is that of $[Ru(bipy)_3]^{2+}$ ($8 \leq 10^{-6}$ mol dm^{-3}) for comparison.

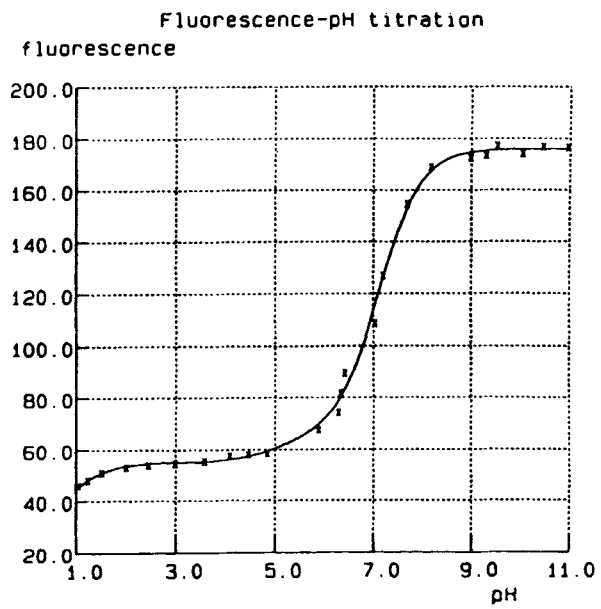

Figure 3 Fluorescence pH titration of 1,4,7-tris{bis(2′,2″-bipyridyl)(2′,2″-bipyridyl-5′-ylmethyl)ruthenium(II)}-1,4,7-triazacyclononane (L^{26}; 2×10^{-6} mol dm^{-3}). The data were fitted to equation (1) to give the calculated curve shown.

Table 1 Comparison of the photo excited-state pK_a values of the macrocycles L^{10} and L^{25}–L^{27}, determined at 25 °C by fluorimetric and uv-visible pH titration respectively, with the literature ground-state values for the parent macrocycles *cyclam* (14N4) and 1,4,7-triazacyclononane (9N3) determinded by acid-based or NMR pH titration.

Ligand	*Overall charge*	pK_1	pK_2	pK_3	pK_4	*Method*
cyclam	0	11.5	10.2	1.6	0.9	pH titre
L^{10}	2+	10.29 ± 0.32	9.97 ± 0.13	4.12 ± 0.23	-0.3 ± 0.8	Fluorescence
L^{25}	4+	10.58 ± 0.14	6.89 ± 0.24	3.48 ± 0.29	0.57 ± 0.36	Fluorescence
L^{25}	4+	10.27 ± 0.03	7.45 ± 0.06	5.49 ± 0.34	1.15 ± 0.27	Visable[a]
L^{27}	8+	5.92 ± 0.11	4.78 ± 0.06	2.87 ± 0.18	0.50 ± 0.18	Fluorescence
L^{27}	8+	7.84 ± 0.04	5.27 ± 0.08	3.67 ± 0.06	0.86 ± 0.13	Visible[a]
9N3	0	10.4	6.8	< 2.5		NMR
L^{26}	6+	7.14 ± 0.03	5.04 ± 0.33	0.71 ± 0.31		Fluorescence
L^{26}	6+	6.93 ± 0.11	3.43 ± 0.24	1.43 ± 0.75		Visible[a]

[a]Ground state pK_a values. The changes in the visible spectra with pH are rather small, leading to less reliable values unless multiwavelenth data are used.

excess H^+, Ni^{2+} or Cu^{2+} are added to $[Ru(bipy)_3]^{2+}$ alone, but similar behaviour to that shown for L^{27} is also observed for L^{10}, L^{25} and L^{26}.

A pH fluorescence titration curve for L^{26} is shown in **Figure 3**. Data from this titration curve were fitted to equation (1) to give three photo excited state pK_a's. The calculated fluorescence curve (F) is compared with the observed data (F_{obs}) in **Figure 3**.

$$F/L_T = \frac{F_L + F_{HL}10^{(pK_1 - pH)} + F_{H_2L}10^{(pK_1 + pK_2 - 2pH)} + F_{H_3L}10^{(pK_1 + pK_2 + pK_3 - 3pH)}}{1 + 10^{(pK_1 - pH)} + 10^{(pK_1 + pK_2 - 2pH)} + 10^{(pK_1 + pK_2 + pK_3 - 3pH)}} \quad (1)$$

In equation (1), F_L, F_{HL}, and $F_{H_2}L$ are the intrinsic molar fluorescence values for the unprotonated, mono- and di-protonated ligand respectively, and L_T is the total ligand concentration. Observed data were fitted to equation (1) using non-linear least-squares, refining the three molar fluorescence values and the three pK values. The pK values are collected for L^{26}, together with those for the other fluorescent sensors so far investigated, in **Table 1**.

The appropriate equations analogous to equation (1) were used in each case. As is evident from **Figure 3**, the first photo excited state pK_a of L^{26} is optimal for use of this ligand as a sensor at physiological pH. The first protonation results in the greatest change in fluorescence, and since the first photo excited state pK value is 7.14, the maximum fluorescence change occurs very close to pH 7. Like L^{26}, the more highly charged pH sensor L^{27} shows the greatest fluorescence change on first protonation. L^{27} has a first photo excited state pK_a (pK_1) of 5.71, making it possible to study reactions of this ligand in aqueous solution by fluorimetry without having to take into account protonated ligand species. With L^{10} and L^{25}, lowering the pH causes the fluorescence to first decrease, then increase, before decreasing again. The largest fluorescence changes for these two ligands occur below pH 2, when the N-atoms carrying the pendent $[Ru(bipy)_3]^{2+}$ arms become protonated. As expected, initial protonation occurs at the NH-groups not carrying a pendent arm, and this gives rise to rather small (but measurable) fluorescence changes. The effect of adding increasing numbers of pendent $[Ru(bipy)_3]^{2+}$ arms to both *cyclam* and 9N3, which increases the overall charge on the unprotonated macrocycles from 2+ to 8+, is seen from the data in **Table 1** to gradually lower the pK values as expected. Comparison of the ground state pK_a values of *cyclam* with the photo excited state pK_a values of L^{27} shows pK_1 is lowered from 11.5 to 5.7, and pK_2 from 10.2 to 4.55 due to the 8+ charge on the latter. For L^{26}, the values of pK_1 in the ground and photo excited states are approximately the same within experimental error.

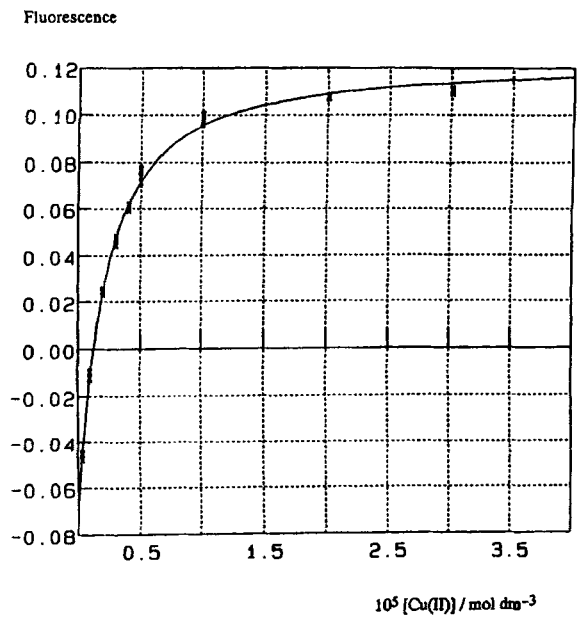

Figure 4 Fluorescence titration curve for the reaction of $[Cu(H_2O)_6]^{2+}$ with 1,4,8,11-tetrakis{bis(2',2''-bipyridyl)(2',2''-bipyridyl - 5'- ylmethyl)ruthenium(II)}- 1,4,8,11 - tetraazacyclotetradecane (L^{27}; 2 ≤ 10^{-6} mol dm^{-3}; pH 6.5; μ = 10^{-3} mol dm^{-3}).

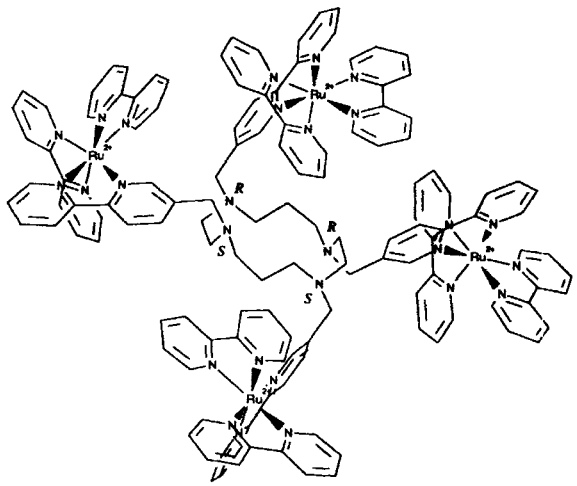

Figure 5 Molecular structure of L^{27} as predicted by molecular mechanics and dynamics calculations using *Hyperchem Version 3*.

Similar behaviour has been reported recently for calixarenes with $[Ru(bipy)_3]^{2+}$ pendent arms.[14]

A fluorescence titration curve for the reaction of $[Cu(H_2O)_6]^{2+}$ with L^{27} is shown in **Figure 4**. These data were analysed to determine the stability constant (log K = 6.01 at 25°C, μ = 0.001 mol dm^{-3}).

Like the protonation constants pK_1 and pK_2, the stability constant has been reduced markedly by attachment of the four $[Ru(bipy)_3]^{2+}$ arms to the N-atoms of *cyclam* (for the parent macrocycle, log K = 24.7). A reduction in the stability constant by 18 orders of magnitude compares with the reduction in the value of K_1 for protonation by 6 orders of magnitude. This large difference can be attributed in part to the higher charge and increased size of Cu^{2+} compared with H^+, and also the steric crowding in L^{27}. Molecular modelling of L^{27} was carried out with Hyperchem Version 3, using the molecular mechanics and molecular dynamics features of this software. The minimum energy conformation is shown pictorially in **Figure 5**. *Cyclam* adopts the unusual *R,S,S,R* set of N-configurations. The steric crowding by the four pendent arms is evident from this structure.

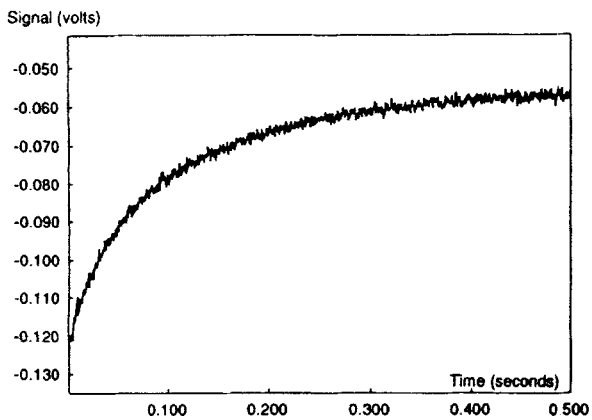

Figure 6 Stopped-flow fluorescence quenching trace showing the rate of uptake of $[Cu(H_2O)_6]^{2+}$ ($4 \leq 10^{-5}$ mol dm^{-3}) by 1,4,8,11-tetrakis{bis(2′,2″-bipyridyl)(2′,2″-bipyridyl-5′-ylmethyl)ruthenium-(II)}-1,4,8,11-tetraazacyclotetradecane (L^{27}; $2 \leq 10^{-6}$ mol dm^{-3}; pH 6.5; μ = 10^{-3} mol dm^{-3}; temperature 25 °C).

Stopped-flow fluorescence kinetic studies of the reactions of L^{27} with $[M(H_2O)_6]^{2+}$ ions (M = Cu, Ni) at pH 6.5 (2,6-lutidine buffer, μ = 10^{-3})

A typical pseudo-first-order stopped-flow fluorescence kinetic trace is shown for the reaction of L^{27} (10^{-6} mol dm^{-3}) with Cu^{2+} (4×10^{-5} mol dm^{-3}) in **Figure 6**. The stopped-flow traces obtained in this way analyse as a single first-order process. Pseudo-first-order rate constants (k_{obs} / s^{-1}) obtained at several Cu^{2+} concentrations were fitted to equation (2) using linear least-squares, to give values for the second-order formation rate constant (k_f / dm^3 mol^{-1} s^{-1}) from the slope, and less accurate first-order dissociation rate constants (k_d / s^{-1}) from the intercept.

$$k_{obs} = k_d + k_f [Cu^{2+}] \quad (2)$$

This gave a kinetically determined stability constant [log (K / dm^3 mol^{-1}) = log(k_f / k_d) = 5.8] which compares favourably with the value of log (K / dm^3 mol^{-1}) = 5.9 obtained from the titration curve (**Figure 4**).

A similar study of the reactions of Ni^{2+} with L^{27} was found to be more complex than that with Cu^{2+} due to the much higher metal concentrations needed to ensure complete complex formation. Plots of the observed pseudo-first-order rate constants (k_{obs}) versus [Ni(II)] increase non-linearly, and this is attributed to a marked salt effect arising from the high charges (8+ and 2+) on the two reactants. The values of k_{obs} were fitted to equation (3):

$$\log(k_{obs}) = \log(k_o) + \frac{1.04 z_A z_B \sqrt{\mu}}{1 + \sqrt{\mu}} \quad (3)$$

This gave a value for the rate constant at zero ionic strength (μ) of log(k_o / s^{-1}) = 0.660 ± 0.002, and the product of the charges on the two reactants of $z_A z_B$ = 9.6 ± 0.1. The latter value is less than the theoretically maximum value of 16, indicating that the 8+ ion L^{27} carries with it a significant number of perchlorate counteranions.

A Tris-(2,2′-bipyridine) chelating azamacrocycle

Ligands L^{28}-L^{30} were investigated by molecular modelling to establish if any of these ligands was capable of forming a mononuclear octahedral tris(2,2′-bipyridine) complex with low-spin, d^6 Fe^{2+} or Ru^{2+}, and if so which of the three ligands was likely to form the most stable complex as judged by the calculated energy minimum.

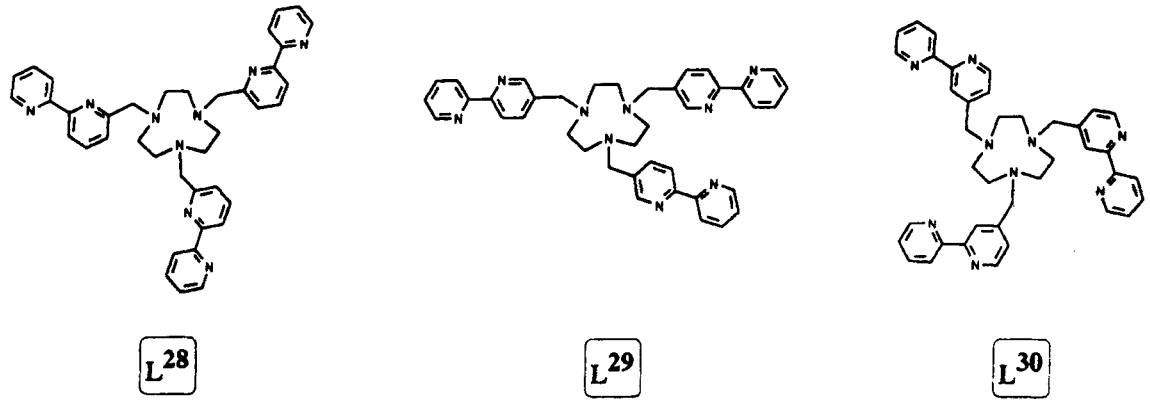

L^{28} L^{29} L^{30}

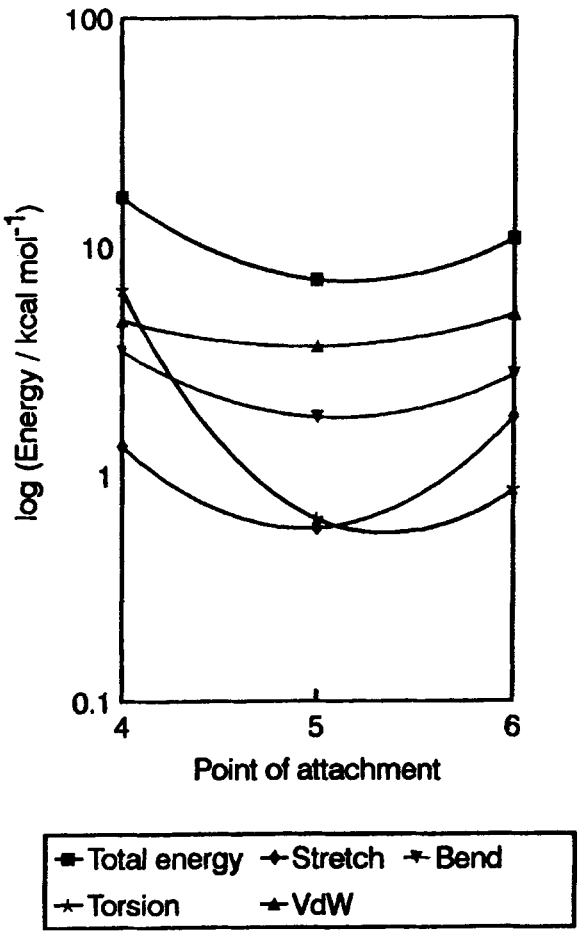

Figure 7 Minimised energy terms from molecular mechanics and molecular dynamics calculations for six coordinate complexes of Fe^{2+} formed by chelation with the three *bipy* arms of L^{28}–L^{30}.

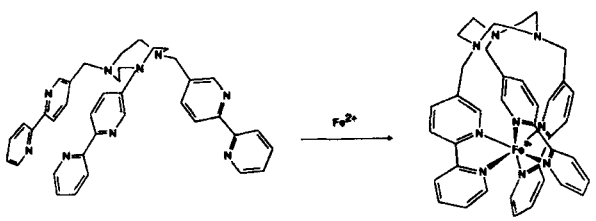

Figure 8 Energy minimised structures of L^{29} and $[Fe(L^{29})]^{2+}$.

L^{28} has been prepared and investigated previously, and the Fe^{2+} complex is reported to be unstable in aqueous solution.[15] The results of the molecular modelling calculations are summarised as a plot of the various energy terms (after minimisation) versus the point of attachment to the *bipy* groups (4, 5 and 6 corresponding to L^{30}, L^{29}, and L^{28}, respectively) in **Figure 7**. It is evident that all of the energy terms are minimised for L^{29}, and that this is the ligand predicted to be the most favourable for octahedral complexation. The energy minimised structure is shown in **Figure 8**.

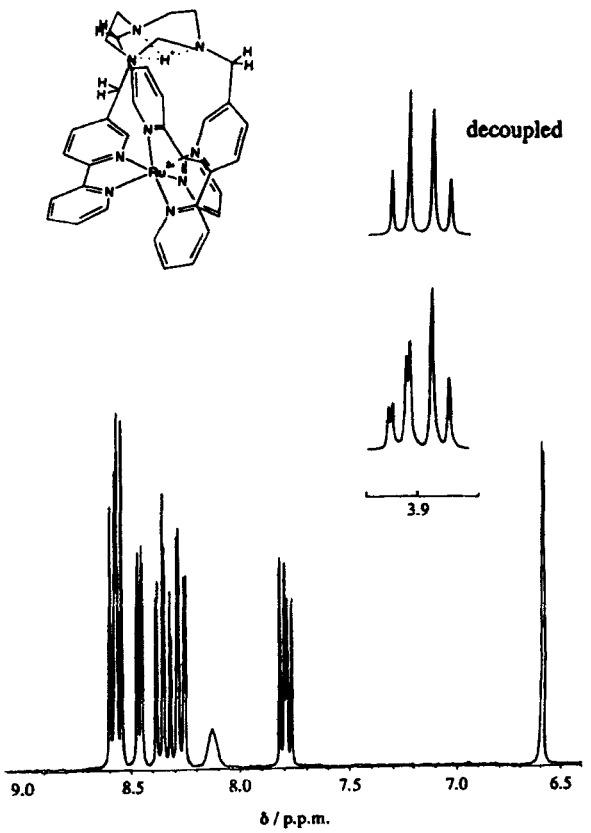

Figure 9 Parts of the ^1H NMR spectrum of $[Ru(L^{29}H)]^{3+}$ showing the proton coupling between the NH^+ proton and the two protons of the linking N-CH_2 groups (an AB quartet; inset).

Also shown in **Figure 8** is the structure predicted by molecular modelling for the uncomplexed macrocycle, which shows the *pre-organised* nature of the ligand, and the relatively small conformational changes that the macrocycle must undergo in forming an octahedral complex. Therefore, we proceeded to synthesise $\mathbf{L^{29}}$ and to examine the complexes it forms with Fe^{2+}, Co^{2+}, Ni^{2+}, Cu^{2+}, Zn^{2+} and Ru^{2+}. The complexes were isolated as $[M(\mathbf{L^{29}H})][PF_6]_3$ salts, indicating a single proton is attached to the ligand. The ^1H NMR spectrum of the Ru^{2+} complex (**Figure 9**) shows the complex is highly symmetric, and reveals the presence of a broad resonance around δ 8.13 ppm attributed (from the integral) to be a single trapped proton. This was confirmed by decoupling at the frequency of this proton, when the resonances from the methylene groups linking the *bipy* arms to the macrocycle collapse into the normal AB quartet (**Figure 9**). The undecoupled spectrum shows a strong *trans*-coupling between the trapped proton and one proton of the CH_2 group, with a weaker *cis*-coupling to the second proton.

A single crystal X-ray structure of $[Ru(\mathbf{L^{29}H})]^{3+}$ is shown in **Figure 10**. The structure is very close to that predicted by the molecular modelling calculations, and clearly shows that the macrocyclic N-atoms are non-coordinating. The single proton is trapped in the cavity occupied by the macrocyclic N-atoms, and all attempts to remove it have so far failed. An NMR experiment was carried out in 0.1 mol dm^{-3} NaOD in D_2O, and loss of the trapped proton does not occur even after prolonged heating at 70 °C.

Azamacrocycles with 2,2′:6′,2″-terpyridyl pendent-arms

The potentially nonadentate macrocycle $\mathbf{L^{14}}$ (R = C), analogous to $\mathbf{L^{29}}$ but with three *terpy* pendent-arms, has been isolated, and its complexes with lanthanide ions are under investigation. Molecular modelling of the Eu^{3+} complex indicates that this ligand is capable of forming a nine-coordinate structure. The energy minimised structure is shown in **Figure 11**. The ^1H NMR spectrum of the diamagnetic La^{3+} complex is consistent with a highly

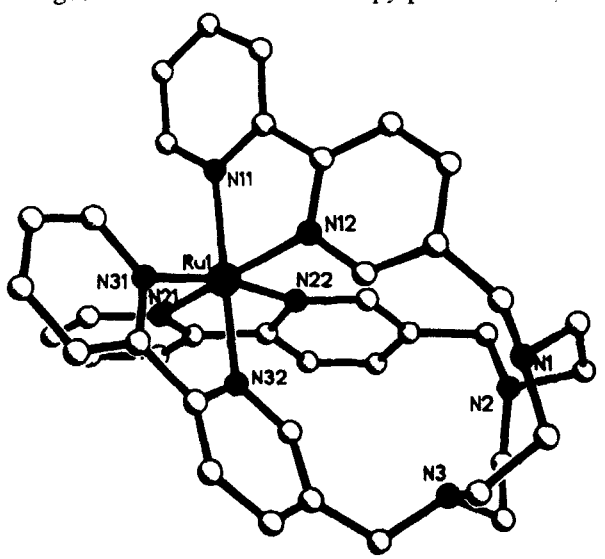

Figure 10 Crystal structure of $[Ru(\mathbf{L^{29}H})]^{3+}$.

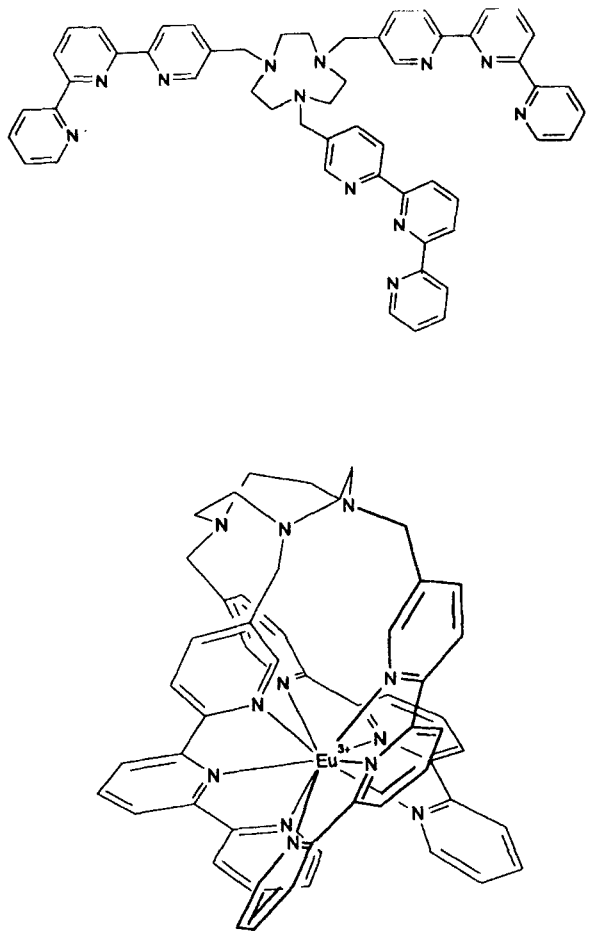

Figure 11 Predicted structure of $[Eu(\mathbf{L^{14}})]^{3+}$ (R = C) from molecular mechanics and molecular dynamics calculations.

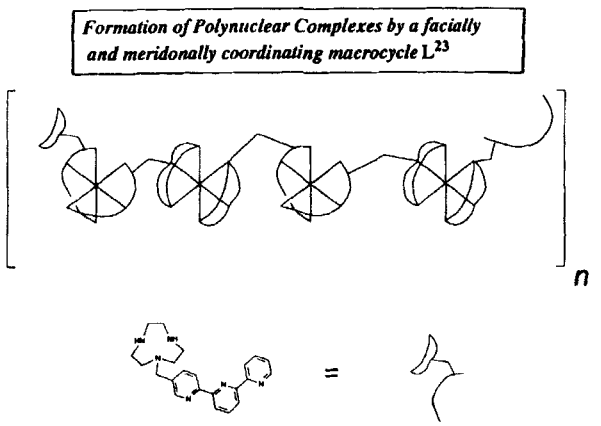

Figure 12 Formation of polynuclear chains by the facially and meridonally coordinating macrocycle *terpy*-CH_2-9N3, $\mathbf{L^{23}}$.

symmetric complex of the type predicted, but confirmation of this must await a crystal structure.

The ligands $\mathbf{L}^{23}$ and $\mathbf{L}^{24}$ which carry a single pendent *terpy* arm have also been isolated. $\mathbf{L}^{23}$ is especially interesting since the 9N3 moeity is facially coordinating, and the *terpy* arm is meridonally coordinating. With six coordinate metal ions, this can be expected to give rise to a degree of self assembly in polynuclear structures of the type shown schematically in **Figure 12**.

With $\mathbf{L}^{23}$ the picture is a little more complicated than that predicted in **Figure 12**, since *cis*- and *trans*-links are possible at the metal centres, although this can be partly overcome by linking the *terpy* arm to the 9N3 at the 4′-position of the *terpy*. Studies of such systems are now under investigation.

ACKNOWLEDGEMENTS

We thank the SERC for financial support of this research, and for the provision of NMR and X-ray facilities, and Dr M. Ward for advice on the synthesis of 5-methyl-2,2′:6′,2″-terpyridine.

REFERENCES

1 F. McLaren, P. Moore and A. M. Wynn, *J. Chem. Soc., Chem. Commun.*, **1989**, 798–800.
2 N. W. Alcock, A. C. Benniston, P. Moore, G. A. Pike and S. C. Rawle, *J. Chem. Soc., Chem. Commun.*, **1991**, 706–708.
3 S. C. Rawle, A. J. Clarke, P. Moore and N. W. Alcock, *J. Chem. Soc., Dalton Trans.*, **1992**, 2755–2757.
4 N. W. Alcock, F. McLaren, P. Moore, G. A. Pike and S. M. Roe, *J. Chem. Soc., Chem. Commun.*, **1989**, 629–632.
5 S. C. Rawle, C. J. Harding, P. Moore and N. W. Alcock, *J. Chem. Soc., Chem. Commun.*, **1992**, 1701–1703.
6 H. A. A. Omar, P. Moore and N. W. Alcock, *J. Chem. Soc., Dalton Trans.*, **1994**, 2631–2635.
7 N. W. Alcock, K. P. Balakrishnan and P. Moore, *J. Chem. Soc., Dalton Trans.*, **1986**, 1743–1745.
8 S. C. Rawle, P. Moore and N. W. Alcock, *J. Chem. Soc., Chem. Commun.*, **1992**, 684–687.
9 P. Sheldon, S. C. Rawle, P. Moore and N. W. Alcock, unpublished work.
10 N. W. Alcock, A. C. Benniston, S. J. Grant, H. A. A. Omar and P. Moore, *J. Chem. Soc., Chem. Commun.*, **1991**, 1573–1575.
11 N. W. Alcock, K. P. Balakrishnan, P. Moore and H. A. A. Omar, *J. Chem. Soc., Dalton Trans.*, **1987**, 545–550.
12 S. J. Grant, P. Moore, H. A. A. Omar and N. W. Alcock, *J. Chem. Soc., Dalton Trans.*, **1994**, 485–489.
13 M. L. Turonek and P. Moore, unpublished work.
14 R. Grigg, J. M. Holmes, S. K. Jones and W. D. J. A. Norbett, *J. Chem. Soc., Chem. Commun.*, **1994**, 185–187.
15 R. Ziessel and J-M Lehn, *Helv. Chim. Acta*, **1990**, **73**, 1149–1162.